Landscape and Landforms of the Samoti Plain, Eritrean Danakil

6

Paolo Billi

Abstract

The Samoti plain is a structural basin and it is located in the northern part of the Danakil depression. The environment is that typical of a hot and dry desert. The landscape has been shaped by the recent tectonic activity and by hydromorphological and aeolian processes. The rivers are ephemeral and have a dry bed for the most of the time. Data on channel morphology and bed material grain size were collected in the field. An abrupt change from a boulder to a prevailing sandy bed was found to occur within a very short distance (about 100 m), and an explanation based on the abrupt decline of shear stress for water infiltration is presented. The prevailing type of wind dunes is the transverse dunes, originated from the coalescing of barchan dunes. The wavelength and the wavelength-to-height ratio of the Samoti plain dunes are smaller and higher, respectively, compared to the dunes of other larger deserts in the world. An explanation based on the limited sediment supply in the windward side of the Samoti plain is discussed. Several elements observed in the basin infilling sediment indicate that the Samoti plain was subjected to a wetter climate around 7–5000 years BP in coincidence with the African Humid Period.

Keywords

Structural basin • Ephemeral streams • Distributary systems • Wind dunes • Dryland

6.1 Introduction

The Danakil is a long and narrow depression of structural origin. It is about 300 km long and less than 42 km wide south of the Gulf od Zula, to become wider and wider southward as far as the Afar region. The Eritrean portion of the Danakil is only about 100 km long, but similarly to the southern portion, it is characterized by impressive landscapes and landforms witnessing their origin from erosion and deposition processes that have accompanied the complex tectonic and volcanic events, which have affected this area since the Neogene (Abbate et al. 2004). Though the Eritrean Danakil is separated from the Red Sea by a low mountain range and lines of recent volcanoes, not exceeding 645 and 371 m asl, respectively, the ground in the central part of this structural depression is commonly below sea level (−100 m in the southern portion and −20 m in the Samoti plain, in the northern part). The Eritrean Danakil is one of the hottest and driest inhabited places in the world. In the Samoti plain, the maximum temperatures range from 44 °C, in winter, to over 50 °C, in summer, and annual precipitation is probably less than 150 mm. This chapter reports about the geomorphological landscape of the Samoti plain, and in particular, it deals with the modern fluvial and eolian landforms and processes.

6.2 Study Area

The Samoti plain takes up the bottom of a depositional, structural basin oriented parallel to the Red Sea. It is located within the Eritrean Danakil depression, about 36 km southeast of the Gulf of Zula. The Samoti plain is famous for the finding of one million years old *Homo* erectus bones (Abbate et al. 1998) (Fig. 6.1). The basin is actually divided into two portions by the recent (Pleistocene to Holocene) emplacement of a large extensions of ryholitic and basaltic lava emitted from the volcanoes of the Alid group when a

P. Billi (✉)
International Platform for Dryland Research and Education, Tottori University, Tottori, Japan
e-mail: bli@unife.it

P. Billi (ed.), *Landscapes and Landforms of the Horn of Africa*, World Geomorphological Landscapes,
https://doi.org/10.1007/978-3-031-05487-7_6

much larger structural basin was already formed. These volcanoes are placed on the eastern master fault that likely originated the larger structural basin, which virtually includes also the Gulf of Zula, stretching for about a length of 100 km. The larger basin is now fragmented in 3–4 portions by transverse faults and by the basalt flows that have reached the center of the basin and in places have reached the Pleistocene deposits on the other side of the basin, of which the latter are an older filling. Here, the recent (probably Holocene—Sani et al. 2017) lava flows of the Alid group have split the Samoti plain into a northern and a southern portion (Figs. 6.1 and 6.2).

A simplified sketch of the geology and stratigraphy of the northern portion of the Danakil depression area is reported in Fig. 6.2; a focus on the main geological characteristics of the Samoti plain is outlined in Figs. 6.3 and 6.4.

Unfortunately, no meteostation is available in the study area. The nearest ones are on the Red Sea coast: Mersa Fatma, 38 km ENE of the study area, Massawa, about 115 km to the NNW (Fig. 6.2) and Assab, which is rather far south (340 km), but it is the only meteostation with some wind data. In a similar inland position, there is Dallol, in Ethiopia (Fig. 6.2), but its climatic data are very old (Pedgley 1967). Nevertheless, also the data of Dallol were considered in order to give a more comprehensive information about the climate of the study area.

The temperatures in the Samoti plain are very high during any season (Fig. 6.5). The hottest temperatures are recorded in summer with mean monthly maximum values close to 40 °C in Massawa and Mersa Fatma e over 45 °C in Dallol, where peaks of 58 °C have been recorded. In the Samoti plain, the author of this paper has measured maximum daily temperatures of 42–44 °C in November 2007. Such hot temperatures are due to the inland position and the occurrence of a coastal range that prevent this area from the refreshing action of the sea, as it is instead observed in the coastal towns of Massawa, Mersa Fatma, and Assab. Also, the mean monthly lower temperatures are relatively high with a lower value around 25 °C in January and the highest values around 31–32 °C in the summer at Dallol. In the other meteostations, the minimum temperatures are on average 5–7 °C lower than in Dallol. In November 2007, in the Samoti plain, temperatures around 30 °C in the night and 25–26 °C at dawn were measured by the author of this paper.

Rainfall is very unusual in Dallol (a few millimeters per year) and in the Samoti plain as well, though the closer vicinity with the basin western shoulder mountains, with peak between 1800 and 2000 m asl, may favor the development of orographic rains reaching also the Samoti plain. The annual precipitation, however, is expected to be less than 100 mm. In Massawa annual rainfall is 186 mm, in Mersa Fatma 238 mm, and in Assab 71 mm. The higher monthly rain occurs at the end of autumn and in winter (Fig. 6.6). In all the weather stations considered in this study, with the exception of Dallol, the average monthly rain is typically less than 10 mm.

The only wind data available are from the meteostation of Assab. These data cover only a few years and are the only information on the wind regime based on field measurements for the study area. Nevertheless, the wind data available are useful to give even a rough an idea of the

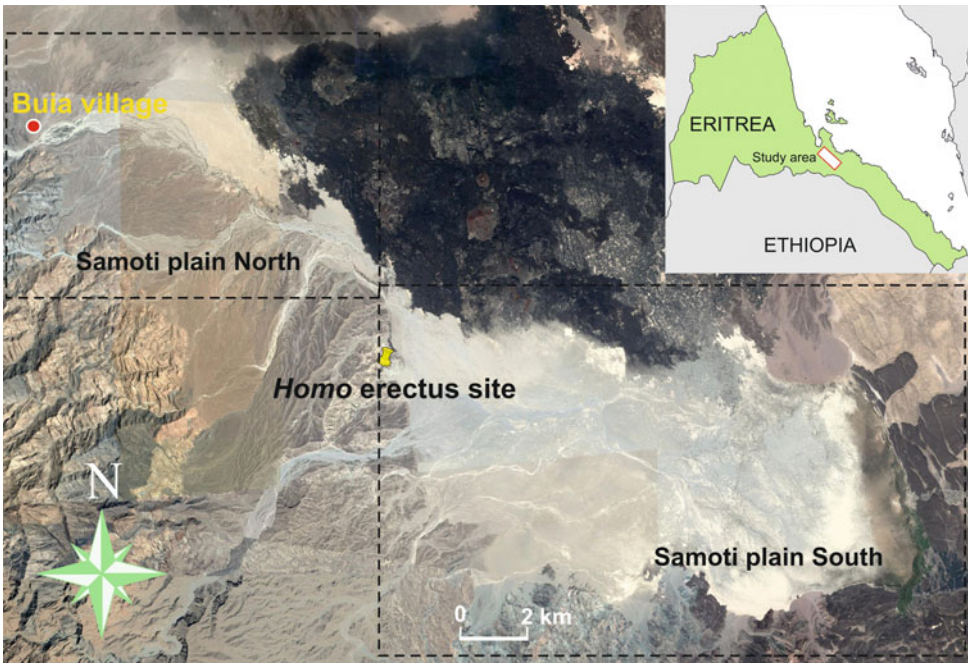

Fig. 6.1 Location map of the Samoti plain. For a more detailed geomorphological map of the northern and southern portions, see Figs. 6.3 and 6.4, respectively. The yellow pin indicates the *Homo* erectus site

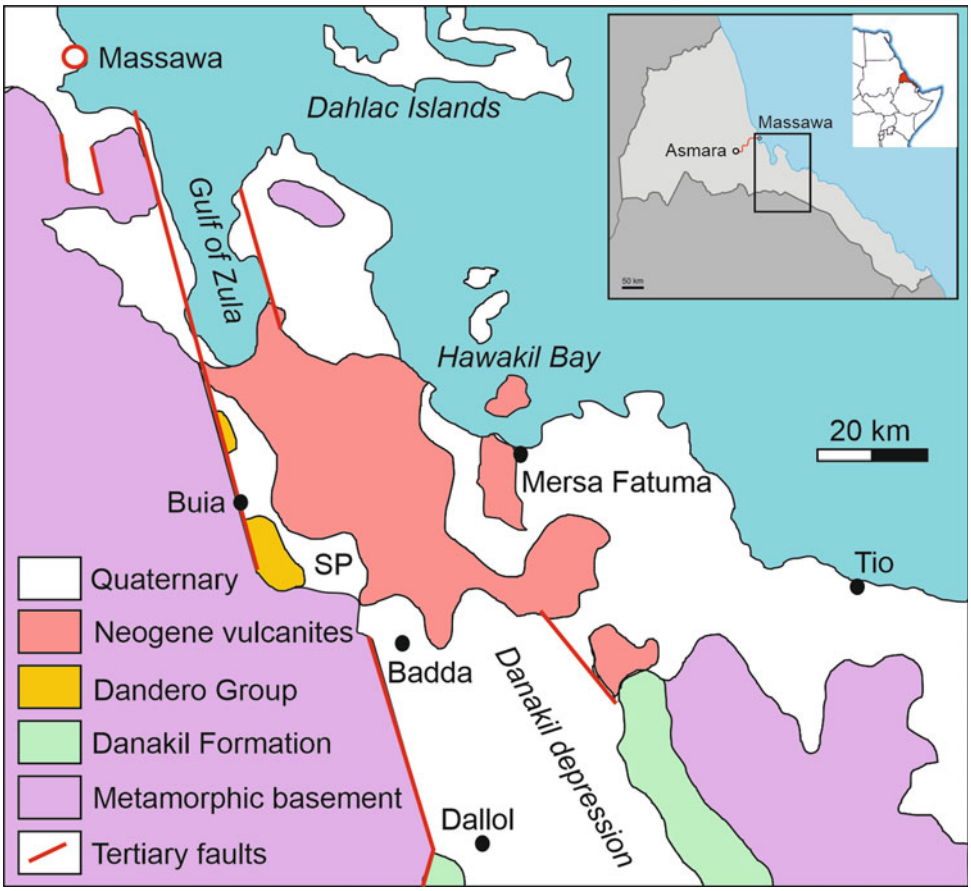

Fig. 6.2 Sketch geological and stratigraphic map of the northern portion of the Danakil depression. SP stands for Samoti plain. The basement rocks include Neoproterozoic and Paleozoic slates, marbles, metadolostones, chloritoschists, sandstones, and limestones; the Danakil formation includes Miocene to Pliocene sandstones and shales; the Dandero group consists of Early to Middle Pleistocene fluvial, fluvio-deltaic and lacustrine to palustrine sand and gravel deposits; the Neogene vulcanites are mainly rhyolitc lavas, ignimbrites, pumices, and basaltic lava flows and fields [simplified and redrawn from Abbate et al. (2004), Ghinassi et al. (2009), and Sani et al. (2017)]

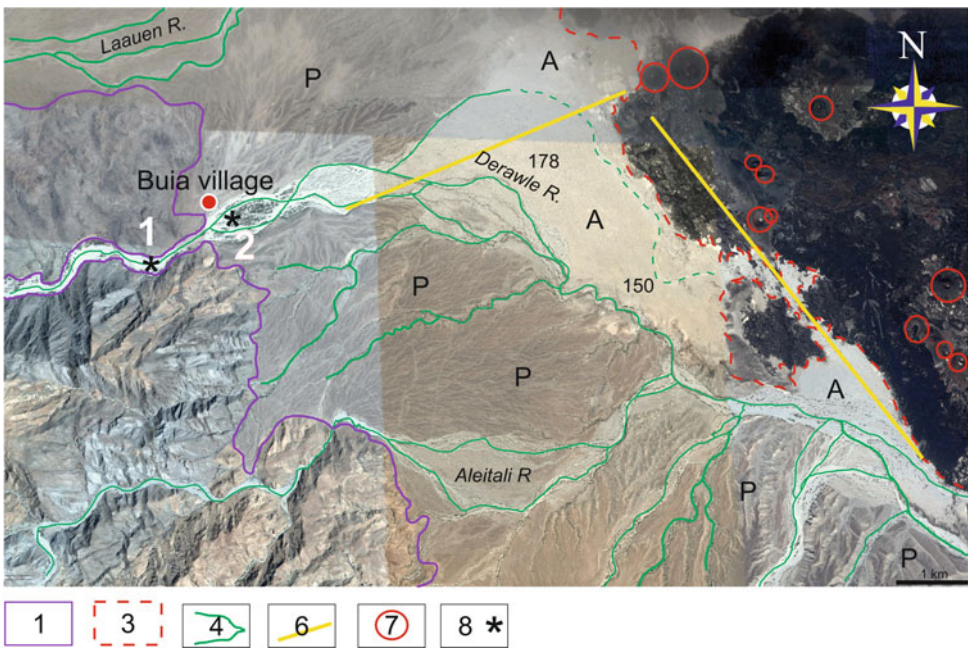

Fig. 6.3 Map of the main geo-lithological and geomorphological elements of the northern portion of the Samoti plain: (1) Neoproterozoic and Paleozoic metamorphic basement; (3) Basaltic lava flows and field (Late Pleistocene-Holocene); (4) ephemeral streams main channels; (6) main faults; (7) volcanic center; (8) bed material sampling site (*) and sample identification number (in white); P = Pleistocene deposits; A = recent alluvial deposits; black numbers indicate the elevation above sea level (modified from Sani et al. 2017)

prevailing wind directions and velocity, which can be considered representative also for the study area. The prevailing winds blow from SE from October to May and in February–March, whereas in November–December, the highest average velocities of 8.5–9.5 ms^{-1} (Fig. 6.7) are recorded. Rosen et al. (1999) compiled a larger number of wind speed

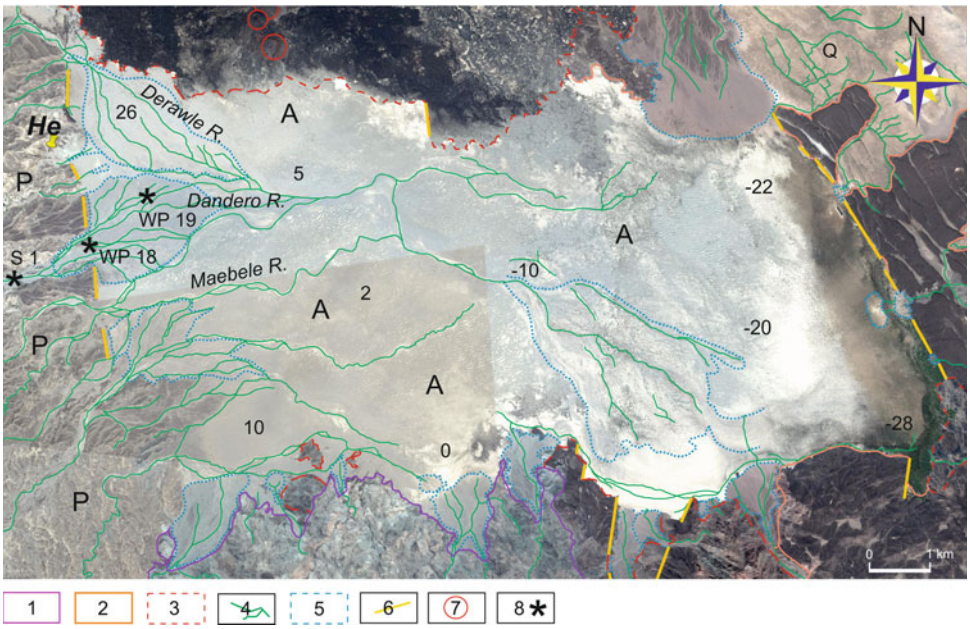

Fig. 6.4 Map of the main geo-lithological and geomorphological elements of the southern portion of the Samoti plain: (1) Neoproterozoic and Paleozoic metamorphic basement; (2) Pliocene–Pleistocene stratoid basalts and subordinately rhyolitic lavas; (3) Basaltic lava flows and field (Late Pleistocene-Holocene); (4) ephemeral streams main channels; (5) distributary systems; (6) main faults; (7) volcanic center; (8) bed material sampling site (*) and identification number; P = Pleistocene deposits; Q = undifferentiated Quaternary deposits; A = recent alluvial deposits; He = the *Homo* erectus site; black numbers indicate the elevation above or below (−) sea level (modified from Sani et al. 2017)

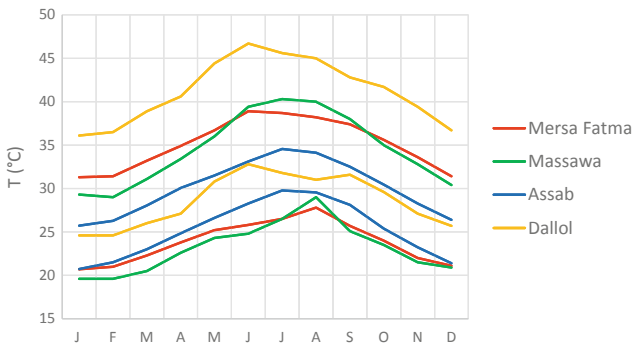

Fig. 6.5 Mean monthly minimum and maximum temperatures measured at selected meteostations near the study area

observation recorded every three hours at the Assab airport and archived by the United States Air Force Environmental Technical Application Center. Their frequency distribution diagram indicates that wind velocities higher than 10 ms^{-1} were recorded but their frequency is less than 5% (Fig. 6.8).

The prevailing wind direction from SE, associated with the highest velocities, is consistent with the Khamsin wind, which is not a seasonal nor or a cyclic wind blowing for intermittent long period across the Sahara. Khamsin is an Arab word that means 50, i.e., the number of consecutive days that, according to the tradition, this wind blows with a certain regularity. Though no wind data in available for the Samoti plain, the local people confirm the occurrence of the

Fig. 6.6 Mean monthly precipitation measured at selected meteostations near the study area

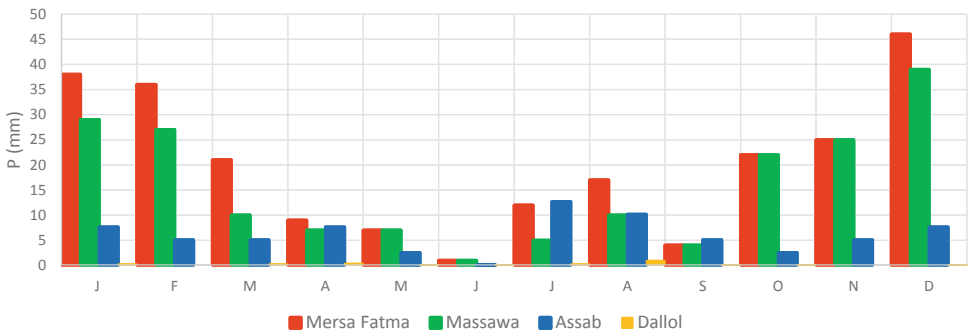

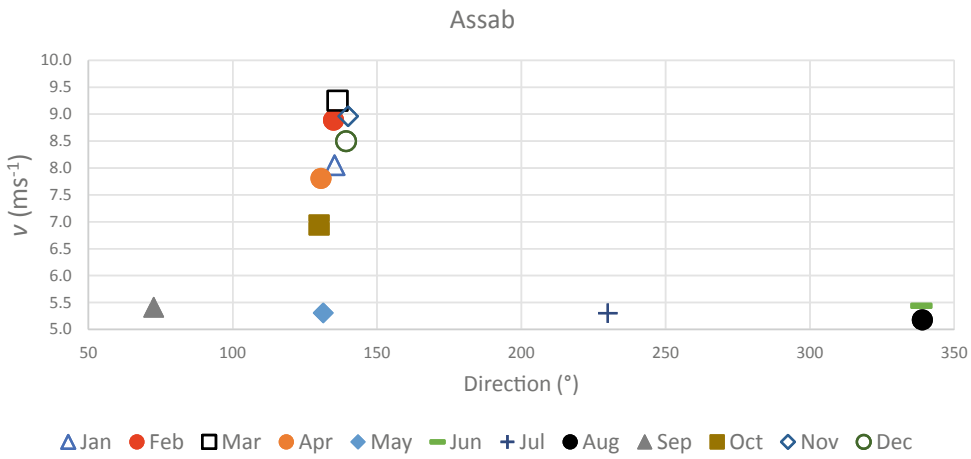

Fig. 6.7 Mean monthly wind velocity measured at Assab

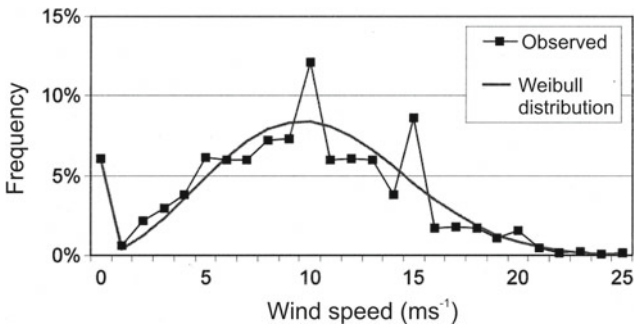

Fig. 6.8 Diagram of wind velocity frequency distribution. Weibull distribution is actually a three-parameter Weibull probability density function (modified from Rosen et al. 1999)

Khamsin, but its blowing duration seems to be shorter, from days to a couple of weeks. This wind is capable to move the fine sediment of the Samoti plain and to form aeolian dunes as it will be illustrated farther on.

Under such hot and dry conditions in any season, a desert environment is not unexpected. The Samoti plain area, in fact, is devoid of vegetation with the exception of sparse bush trees and grass tufts in the dry river beds or in their distributary systems. However, this poor vegetation and the fresh water emerging to the surface as small puddles, especially in areas below sea level, seem to be sufficient for a few desert gazelles (Dorcas) to survive. They are probably the largest wild mammals living today in the Samoti plain.

6.3 Geomorphological Landscapes

The landscape characteristics of the study area are strongly influence mainly by the recent geological events. At larger scale, the Samoti plain is located within the northern portion of the Danakil depression which terminates into the Gulf of Zula graben (Fig. 6.2). This structural basin is separated from the Badda basin and the main portion of the Danakil depression by earlier (Pliocene–Pleistocene) volcanic emissions and since then the sedimentary and tectonic evolution of these two grabens followed distinct patterns. The Gulf of Zula graben is markedly asymmetric, with the western shoulder, coinciding with the main escarpment of the Red Sea rift branch, characterized by high elevations close 2000 m asl, from which most of the modern river systems originate. By contrast, the elevations of the eastern horst of the Zula graben are much lower, commonly less than 600 m asl, and only very few small rivers originate from there, impeded in their course development by the Alid volcanoes and their extensive lava emissions. (Fig. 6.9).

In the Zula graben, the river courses run perpendicular to the basin axis in the mountainous escarpment and then, as they reach the garben bottom, they turn into two different axial directions: The northern rivers flow to the north, reaching the Red Sea; the southern rivers flow to the south and end up in the Samoti plain, which is a closed basin (Fig. 6.9). The collapse of the Alid caldera (36–15 ka—Sani et al. 2017) and the following basalt emplacement acted as a sort of divide, thus forcing the main rivers of the Samoti area (Derawle, Aleitali, Dandero, Meeble—Figs. 6.3 and 6.4) to flow southward, in that also favored by the progressive lowering of the southern portion of the Samoti plain bottom, the southwestern part of which has now elevations below the sea level (Fig. 6.4).

The studies of Ghinassi et al. (2009) and of Sani et al. (2017) on the Pleistocene to Holocene deposits filling the Samoti graben depict a complex structural, environmental, and paleogeographic evolution of this area (see Chap. 5 of this publication for more details). The boulder beds topping the filling sequence still preserve their original gradient dipping to NNE (Figs. 6.9 and 6.10), which roughly corresponds to the flow direction of the rivers that formed the entire depositional sequence (about 80 m thick) and that was maintained from the fluvio-lacustrine deposits resting on the basin Neoproterozoic metamorphic basement upward.

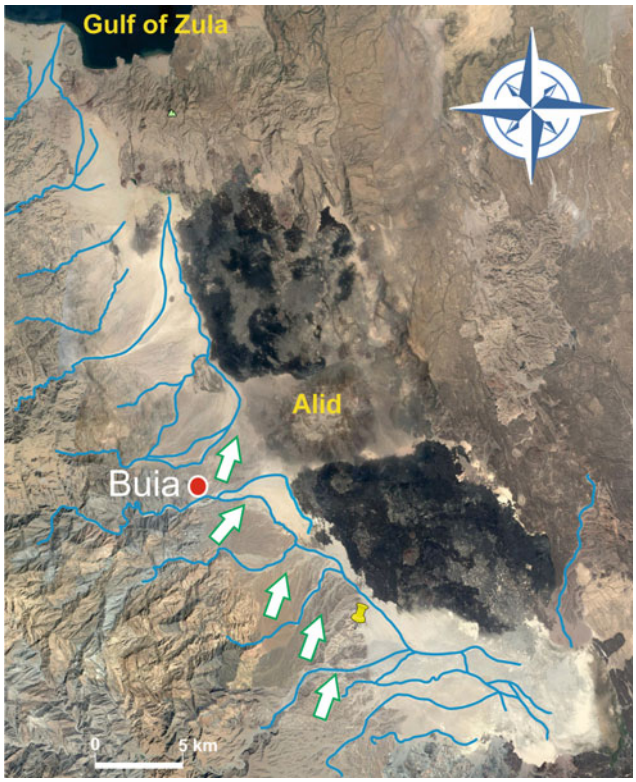

Fig. 6.9 Southern portion of the Gulf of Zula tectonic depression including also the Samoti plain. The recent lava flow of the Alid volcanoes has forced the rivers draining the western margin of the basin in two opposite directions. The white arrows indicate the dip of the Pleistocene fluvial deposits upper surface which correspond to the original depositional gradient (Sani et al. 2017, their Fig. 6) and roughly to the paleocurrents. The yellow pin indicates the *Homo* erectus site

Fig. 6.10 Samoti plain with the flat-topped Pleistocene deposits in the background. The boulder beds on top of the sequence still preserve their original gradient dipping to NNE

As the recent erosion phase started, the Pleistocene deposits were deeply incised by rivers that are still oriented to NNE in the Zula graben north of the Buia, whereas those south of Buia were deflected to the south. This change of flow direction seems to have occurred very recently since one branch of the Derawle river is still flowing to the northeast against the Alid volcano (Fig. 6.11), where it is then deflected to the south. Other channels of the distributary system, formed by the Derawle beyond the narrow valley incised into the Pleistocene deposits, follow a similar pattern.

The rivers entering the Samoti plain form very flat fan-shaped bodies. The alluvial fans that punctuate the plain borders margin (Fig. 6.4) have low gradients, in the 0.005–0.05 range, which are from one to two orders of magnitude lower than dryland fans gradients reported in the literature (e.g., Harvey 2011). The Samoti plain flat fans have morphological characteristics more similar to the distributive systems of ephemeral streams observed in other drylands by Billi (2007). The lack of alluvial fans is probably due to the differential action of the border faults which are probably more active on the eastern margin, resulting in the eastward tilting of the basin bottom and, hence, in the lower elevation of the eastern portion of the plain. Another explanation can be found in the high sedimentation rate and the decreasing accommodation space due to the progressive expansion of the Alid volcanoes toward the center of the basin. In the southern part of the Alid volcanoes, the progradation of the basaltic lavas in the early Holocene (Duffield et al. 1997) reached the opposite margin of the basin, de facto splitting the Samoti plain into a northern and a southern portion (Fig. 6.1). The Derawle river has bypassed the basalt obstruction by cutting a narrow gorge at the contact between the volcanic rocks and the distal outcrops of the Pleistocene deposits (Fig. 6.12).

Throughout the whole study area, desert weathering processes are rather common. Soils are very rare and poorly developed. In places, soil patches may be found on top of alluvial plain deposits, where some overbank flow fine sediment may accumulate (Fig. 6.12). The hill slopes and the flat surface of the Pleistocene deposits are devoid of any kind of soil. They are covered with a rocky weathered mantle forming a typical stone pavement (Fig. 6.13).

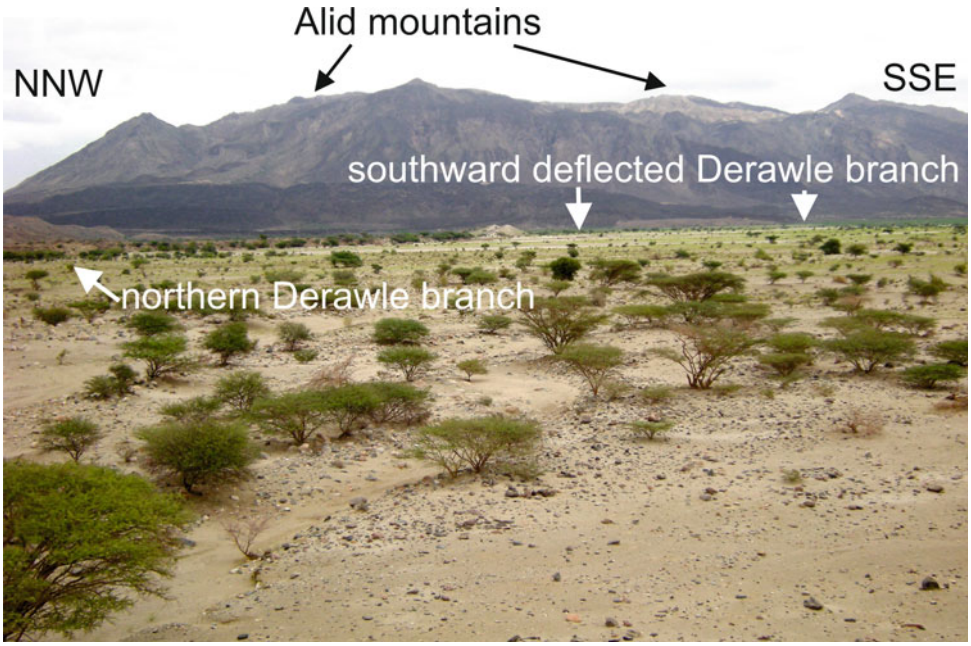

Fig. 6.11 Derawle river distributary system prograding toward the Alid mountains. The northern branch runs to NE along the incision in Pleistocene deposits and reaches out to the Alid mountains, where it is deflected to the south to rejoin the main river channels sharply turned to the south into the Samoti plain

Fig. 6.12 Derawle river downstream of the gorge cut at the contact between the basaltic lava flow prograding to the left (coming from the Alid volcanoes) and the Pleistocene deposits on the right (Google Earth coordinates: 14°47′06″ N–39°56′ 05″ E)

The accumulation of coarse particle on the surface of the Pleistocene deposits plateau is predominantly of primary origin as the coarse particles are the main component of the underlying Boulder bed formation. Here, deflation of fine particles is the prevailing process for the concentration of coarse particle. On the hillslopes underlain by the metamorphic basement rocks or other consolidated sedimentary rocks, weathering processes play a more relevant role in bedrock disintegration (Fig. 6.14), boulder splitting, rock pitting, and alveoles formation (Fig. 6.15). The large availability of sharp-edged rock fragments was an endless supply of raw material for *Homo* erectus to make his tools (Fig. 6.16).

6.3.1 Fluvial Geomorphology and Processes

The rivers entering the Samoti plain are all ephemeral. Water flows only in response to heavy downpours in the headwaters, close to the continental divide between the Red Sea and the Mediterranean drainage systems. Here, the monthly precipitation in June and July can be around 150 mm. On the base of data on dryland rivers in different parts of the world, Kempf et al. (2018) defined an empirical relation between catchment area and event precipitation according to which in the most of the study area rivers 25 mm of rain are necessary to generate some flow. The same authors indicate that stream

Fig. 6.13 Stone pavement on the Pleistocene deposits paleo depositional surface. Notice the absence of soil, the exfoliation on the boulder in the foreground, and the typical black and red desert varnish coating the most of surface stones

flows 0–5 and 3–11 times per year in hyper-arid and semi-arid environments, respectively.

On the coast, the three wettest months are in winter (December-February), but the average monthly precipitation ranges between 25 and 45 mm, and, seldom, they can generate some stream flow in the Samoti plain rivers. From these considerations, it is evident why the study area rivers are dry for most of the time, and though there is no instrumental data of river flow, floods are expected to be rather infrequent.

In the basin western shoulder, rivers have cut deep and narrow valleys and show the typical features of mountain streams; that is, no or a very small alluvial plain is present, the streambed takes up the whole valley bottom, coarse sediment is supplied directly to the stream channel from the hillslopes, bed material is very coarse, and gradients are steep (Fig. 6.17), typically in the 0.03–0.02 range.

As the rivers exit the basin shoulder narrow valley, they enter the Pleistocene deposits in which they have cut wider channels (for instance, the Derawle average streambed width is 561 m, which is more than three times the width of the river in the upstream mountain reach), given the weaker resistance to erosion of these loose sandy and gravel sediments. In these middle reaches, the streambed gradient decreases to values ranging from 0.014 to 0.018 and the rivers assume the typical braided channel morphology (Fig. 6.18). However, bed material is still coarse.

As the rivers proceed beyond the Pleistocene deposits reaches, they enter the basin bottom and form large distributary systems. The distributary channels gradient tends to decrease further, compared to the upstream middle reaches, but the change is less marked as it ranges from 0.015 to 0.009 (see also Table 6.1). Notwithstanding such a relatively small change in gradient, bed material grains size decreases remarkably and the transition from coarse cobbles dominated to sandy bed occurs within a very short distance (for example, no more than 100 m in the Dandero river) (Figs. 6.19 and 6.20). In the Derawle and Dandero rivers, bed material D_{50} and D_{90} do not show any significant change between the mountain reach and the lower gradient, middle reaches cut into the Pleistocene deposits (Table 6.1).

In the Dandero river, though the change in streambed gradient from site WP18–WP19 is almost negligible (Table 6.1), all the characteristic diameters show a very

Fig. 6.14 Mudstone rock weathering and blocky boulders formation

Fig. 6.15 Hard rock weathering processes: **a** boulder splitting and exfoliation; **b** rock pitting; **c** alveoles

Fig. 6.16 *Homo* erectus artifacts on a Pleistocene preserved, depositional paleosurface. Hand ax, chopper, and parent stone are all present in one site

marked decrease of about an order of magnitude, whereas the sand content increases to a value (about 82%) typical of sand bed rivers.

Though in textbooks, it is commonly reported that in rivers grain, size declines with distance downstream according to an exponential low (e.g., Robert 2003), field observations (e.g., Sambrook Smith and Ferguson 1995), and flume experiments (Paola et al. 1992; Sambrook Smith and Ferguson 1996; Venditti et al. 2015) demonstrated that the abrupt gravel-sand transition is rather common in rivers. All these authors provided different explanations, including selective deposition, local base level control on excess of sand supply, abrasion/breakdown of fine gravel, change in slope, and a decrease in shear stress. With the exception of the change in slope, that is, not relevant in the case of the study area rivers, the other factors may play some role in the abrupt gravel-sand transition. However, in dryland ephemeral streams, flood water transmission loss, due to infiltration in the downstream reaches, is a common process (e.g., Costa et al. 2012). A marked decrease of discharge, accompanied by a decrease in shear stress, may result is a sudden decline in sediment transport capacity and deposition of the coarser particle, whereas the sand is selectively transported farther downstream.

In a few cases, one or two river channels may continue beyond the distributary systems, some distance beyond which they form another a much less developed and active distributary system or simply terminate as floodouts (Tooth 2000).

Big floods are not common in the study area. Extreme, high intensity rainfall, however, may generate very large floods that occasionally reach the southeastern margin of the Samoti plain. The large floods are characterized by high sediment transport rates that are capable to transport large boulders as far as the basin center. In fact, individual boulders, 100–200 mm in mean diameter, are found on the stream bed and in the basin filling deposits (Fig. 6.21), very far from the upstream reaches and from the gravel-sand transition (Fig. 6.20).

6.3.2 Aeolian Geomorphology

Aeolian processes are very active in the study area, and their most outstanding results are large areas covered by wind-blown dunes in the southern portion of the Samoti plain (Fig. 6.22). These dunes are basically of the crescentic type that coalesced to form transverse dunes (Fig. 6.23) (Lancaster 1995 and 2011). These dunes have a sinuous ridge, perpendicular to the main wind direction and typically form, where wind direction is constant for long intervals as it is the case of the Samoti plain, where strong and weeks lasting wind is predominantly from southeast (locally known as Khamsin) (Fig. 6.7).

In the study area, the transverse dunes have an average wavelength of 36 m (range 19–61 m) and an average height of 1.5 m (range 0.7–3.0 m). These dunes are much smaller

Fig. 6.17 Mountainous reach of the Derawle river incised into the metamorphic basement (Google Earth coordinates: 10°49′16″ N–39°50′22″ E). The blue arrows indicate the flow direction

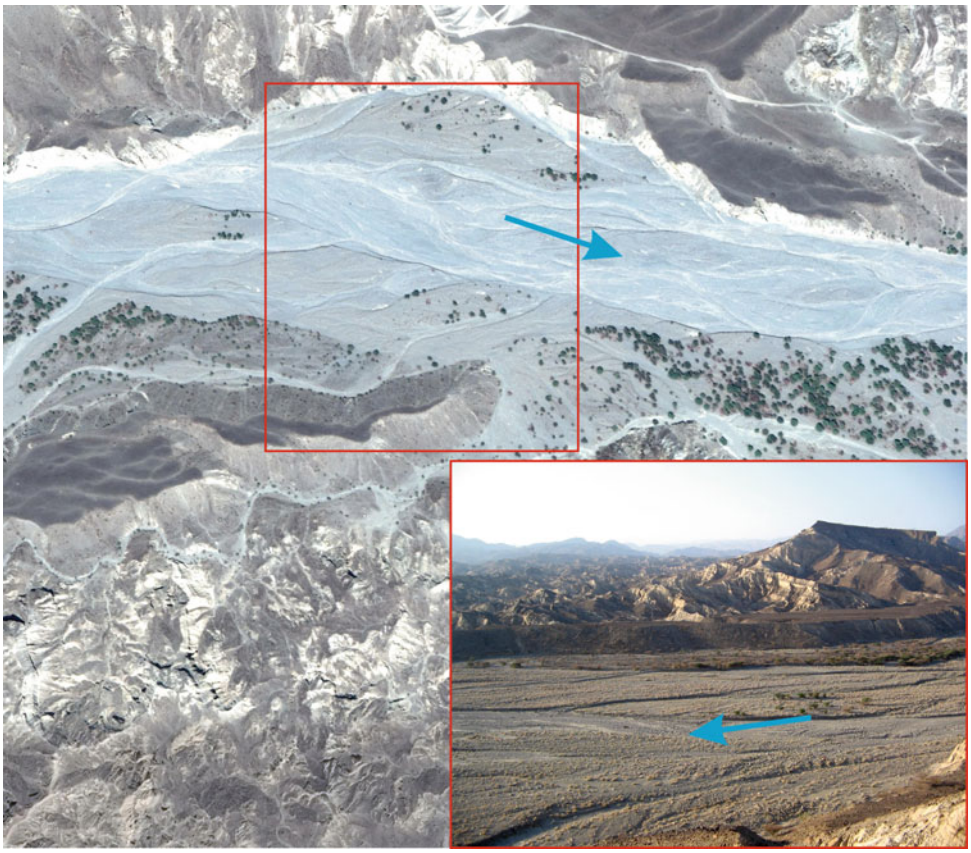

Fig. 6.18 In their middle reaches, cutting through the Pleistocene deposits, the stream bed of the main rivers becomes very large and assumes a braided stream morphology. The braided channel morphology of the Dandero river in the reach is cut into the Pleistocene deposits (Google Earth coordinates: 14°44′32″ N–39°55′56″ E). The blue arrows indicate the flow direction

than those observed in larger deserts, whose wavelength and height vary from 100 to 1000 m and 2–50 m (Fig. 6.24), respectively. The Samoti plain dunes have a larger dune wavelength/height ratio of 24 compared to that of about 5 reported for similar dunes in other deserts of the world (Lancaster 1995). That is, probably due to the limited sediment supply since only very small rivers enter the plain from S-SE-E. The Samoti plain transverse dunes, however, seem

Table 6.1 Main gran size characteristics of bed material in the Derawle and Dandero rivers

River	Site	Gradient	D_{10} (mm)	D_{50} (mm)	D_{90} (mm)	Sand %
Derawle	1	0.026	0.40	1.48	235.3	60.0
	2	0.026	0.31	1.12	181.0	53.6
Dandero	S1	-	0.29	6.35	125.8	44.9
	WP18	0.0012	0.21	7.13	117.1	43.5
	WP19	0.0010	0.08	0.30	22.63	81.7

For sampling site location, refer to Figs. 6.3 and 6.4

Fig. 6.19 Abrupt transition from cobble dominated to sandy streambed in the Dandero river. Flow is toward the reader

to be a smaller scale end member in the great variability of dune size confirming that wind-blown dunes are a classic example of self-organization in a geomorphic system (Hallet 1990). The interdune distance is about 18 m, which corresponds to an interdune area cover of about 50%, a value very close to that of 60% reported for larger dune fields in the world (Lancaster 1995). The interdune area is of deflationary (or non-depositional) dry type (Ahlbrandt and Fryberger 1980; Lancaster 1995). The dunes, in fact, rest and move on a few centimeters thick layer of consolidated muddy sediment (the white parts in Fig. 6.23) which is found all across the most of the Samoti plain southern portion on top of the filling sedimentary sequence.

The dune migration rate was calculated by taking a few shrubs as a fixed reference and comparing Google Earth images of 2011 and 2013. Though the method is not accurate, because many variables could not have been considered, an approximate migration rate of 6 m yr^{-1} was obtained. This value is smaller if compared to larger desert data (Fig. 6.25) (Lancaster 1995), but it is within the range of the global data.

Wind ripples are ubiquitous in any desert and in the Samoti plain as well. Unfortunately, no geometry data for wind ripples are available for the study area, whereas fluvial ripples wavelength and height were measured in the Dandero river. Plotting these data within a wavelength/height bivariate diagram including also wind ripple data from different desert areas in the world (Lancaster 1994) (Fig. 6.26), it is evident that river current ripples cannot be distinguished from wind ripples simply on the base of their geometry, unless for the orientation of the former perpendicular to flow when the direction of the latter is different from that of the prevailing wind.

6.4 Environmental Change

The Samoti plain filling deposits are well exposed for a depth of 2–4 m along the main river channels cut banks. These sediments are predominantly of fluvial origin (Fig. 6.27) and consist mainly of massive, horizontal planar laminate, and cross-bedded sand with silt and clay, thin layers occurring as weathered channel clay plugs (Fig. 6.27) or as a few centimeters (5–30) thick horizontal beds that are mainly found in the upper part of the sedimentary sequence, which is topped by the thickest one. This layer of consolidated clay forms the base on which the wind dune rest and move. No clear evidence of old aeolian deposits was found in the exposed filling sequence.

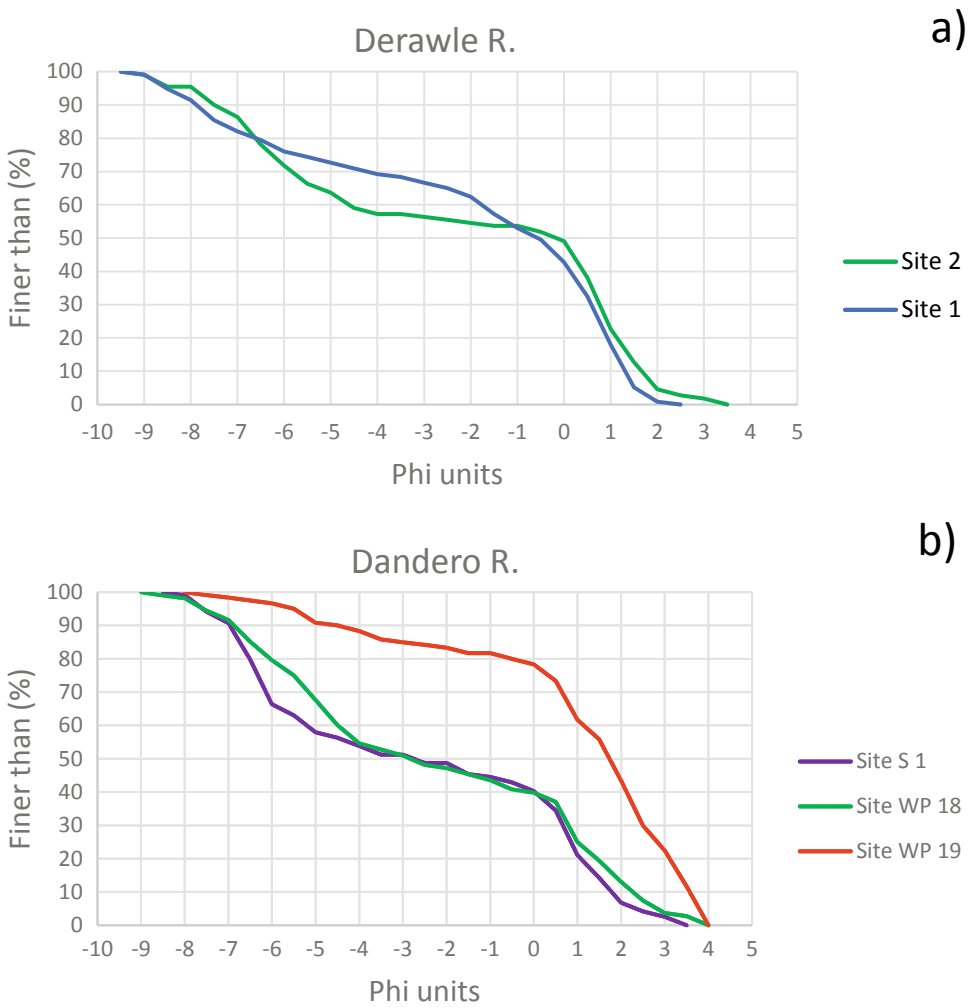

Fig. 6.20 Grain size frequency distribution of the Derawle (**a**) and Dandero (**b**) streambed in different sites (see Figs. 6.3 and 6.4 for the sample location)

Paleochannels range in width from a few meters (Fig. 6.27 a) to about 30 m (Fig. 6.27 b), which is approximately the same width of modern rivers in the study area. The thickness of the weathered clay plug in the largest paleochannel indicates that flow depth was at least 1 m and the redoximorphic features of the channel filling indicate periods of water saturation thus reflecting climate conditions more humid than today. In the modern channels, in fact, fine sediment was observed only as a very thin (1–3 mm thick) drape on the streambed, whereas no soil development on top of the river alluvial deposits where fine sediment deposition from overbank flow should be expected. Moreover, on the upper part of the sequence and on the surface of the top thick muddy layer, there is evidence of saturated sediment deformation (Fig. 6.28a, b) and desiccation mud cracks (Fig. 6.28c). Soft sediment deformation implies water saturation, and two main processes are involved: compaction and/or liquefaction. Compaction is due to overburden, and according to Alsop et al. (2017), also a limited amount of overburden may be sufficient to generate compaction fabrics in unconsolidated sediment. In horizontal beds, however, soft sediment deformation can be considered the result of earthquake-induced liquefaction (Allen 1986).

Some footprints of a big bovidae were found on the top muddy layer (Fig. 6.29). It is not easy to identify the animal that made them but, given the large size of the footprints, for sure they were not made by the gazelles that occasionally can be seen in the Samoti plain. Gazelle expert (Ito, personal communication) suggests that the footprint of Fig. 6.29 could be of a big antelope, the size of a greater kudu, which is a scrub and bush woodland antelope, nowadays found in the Ethiopia and Eritrea highlands, whereas no similar big antelope seems to be present in the study area. In the past, more humid conditions may have favored a denser vegetation cover, likely enough to feed also such a big antelope.

All these elements point at past wetter conditions, probably coinciding with the African Humid Period. During such humid interval, rivers discharge was intermittent but, likely, with longer than today base flows and temporary swamps may have formed in the alluvial plain. As the climate

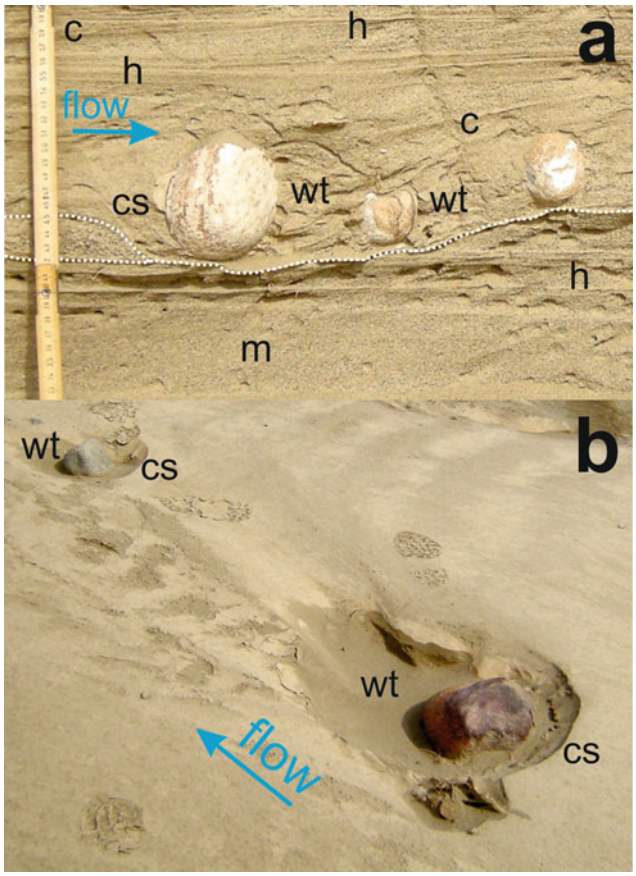

Fig. 6.21 Isolated cobbles within the basin filling sandy deposits (**a**) and on the modern streambed (**b**) in the center of the Samoti plain; cs = crescent scour upstream of the individual boulder; wt = wake turbulence area and disturbed sediment; h = horizontal lamination; c = cross-bedded or inclined lamination; m = massive sand; white dotted line = erosion surface in the massive sand layer under the cobbles

changed, becoming very dry within a relatively short time, conditions were set for the development of the Khamsin wind and the formation of Aeolian dunes. The soft sediment deformation, associated with water saturation and earthquakes, may witness the reactivations of faulting along the Samoti plain with a progressive lowering of its southeastern portion, thus triggering the incision of the modern rivers into the basin filling deposits.

Unfortunately, no dating of this deposits is available, but the most recent of them should be at least Holocene. A humid period is documented for the Sahara (de Menocal et al. 2000; de Menocal and Tierney 2012). It occurred between 10 and 5 yr. ago, and it is witnessed by higher discharges and delta sedimentation rates of the Nile (Sun et al. 2019), higher than present water level in many lakes across Central and Northern Africa (de Menocal and Tierney 2012), including lakes in Ethiopia (e.g., Benvenuti et al. 2002) and by the humidity index (Tjallingii 2008), which show two peaks around 7–6 yr. BP.

According to de Menocal et al. (2000), the early Holocene humidity period ended up abruptly (within a few hundred years—Holmes and Hoelzmann 2017) 5 yr. ago with the onset of very dry conditions. On the base of soil stable isotopic and elemental analyses, radiocarbon dating and historical data, Terwilliger et al. (2011) concluded that in Northern Ethiopia and Eritrea, the interval between 4400 and 1200 kry BP was characterized by increasing aridity interrupted by relatively short wetter periods, though in a context of general rainfall decrease.

Though no dating is available for the Samoti plain filling, it seems reasonable to associate the large river channels with weathered clay plug and the top thick clayey layer with the

Fig. 6.22 Main dune fields of the Samoti plain (areas within the dashed lines). The thick arrows indicate the main directions of potential sediment supply; the thin lines indicate the wind direction and the numbers the angle to the north of their provenance

Fig. 6.23 Satellite and ground view of the crescentic dunes merged into transverse dunes

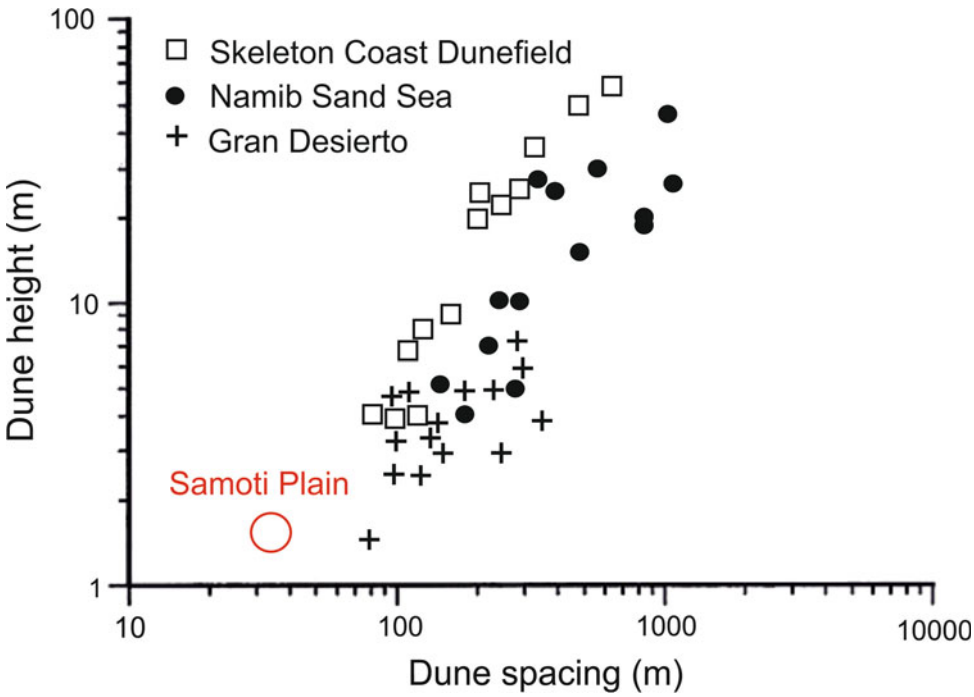

Fig. 6.24 Dune spacing vs. dune height. The Samoti plain dunes are smaller than those in other deserts (modified from Lancaster 1995)

African Humid Period and the formation of the aeolian dunes with the onset of dryer conditions that initiated 5000 years ago.

6.5 Concluding Remarks

The Samoti plain is the floor of a structural basin in the northern part of the Danakil depression. In spite of the sediment filling, the southeastern part of the plain is about 20 m below sea level. The main geomorphological characteristics of the study area reflect the combination of the recent geo-structural events with weathering, erosive, and depositional fluvial and aeolian processes. The climate is hyper-arid. Rainfalls occur mainly on the main Eritrean escarpment, on which the headwaters of the main rivers are located. On the Samoti plain, rains are very sporadic and temperatures are very hot providing the region with the typical characteristics of a desert environment.

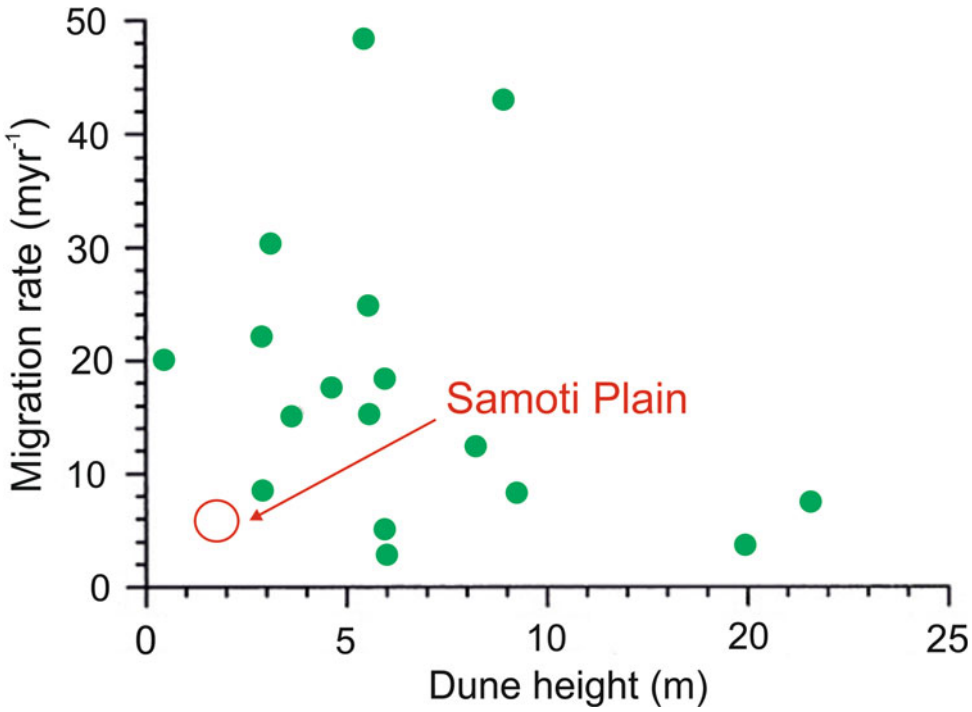

Fig. 6.25 Dune height vs. migration rates. The Samoti plain dunes are smaller and migrate at slower rate compared to dunes of other deserts in the world (modified from Lancaster 1995)

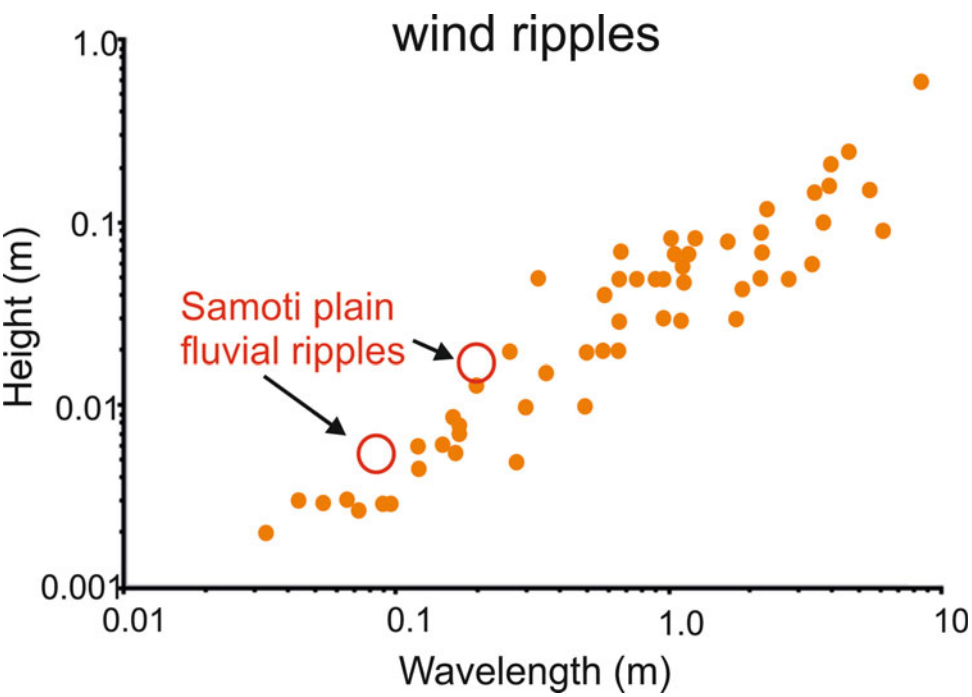

Fig. 6.26 Ripples wavelength vs. height. The fluvial ripples of the Samoti plain rivers cannot be distinguished from wind ripples of different deserts in the world (modified from Lancaster 2009)

The rivers entering the closed basin of the Samoti plain are ephemeral with a dry bed for most of the time. Water flows are resumed only in response to very intense rainstorms, which, occasionally, my turn these dry streambeds into furious rivers. In the mountain valleys and in the middle reaches, the streambed consists of large boulders, but the transition from a very coarse to a prevailing sandy bed material occurs within a very short distance (around 100 m) without a marked change in the streambed gradient. Such a fast transition from coarse gravel to sand has been observed also in rivers of more humid environments, but no specific explanation is shared within the scientific community. In dryland ephemeral streams, however, the high rate of flood water infiltration, especially in the downstream reaches, results in a sharp decrease in discharge. The consequent decrease in shear stress implies a decline of sediment transport capacity and the

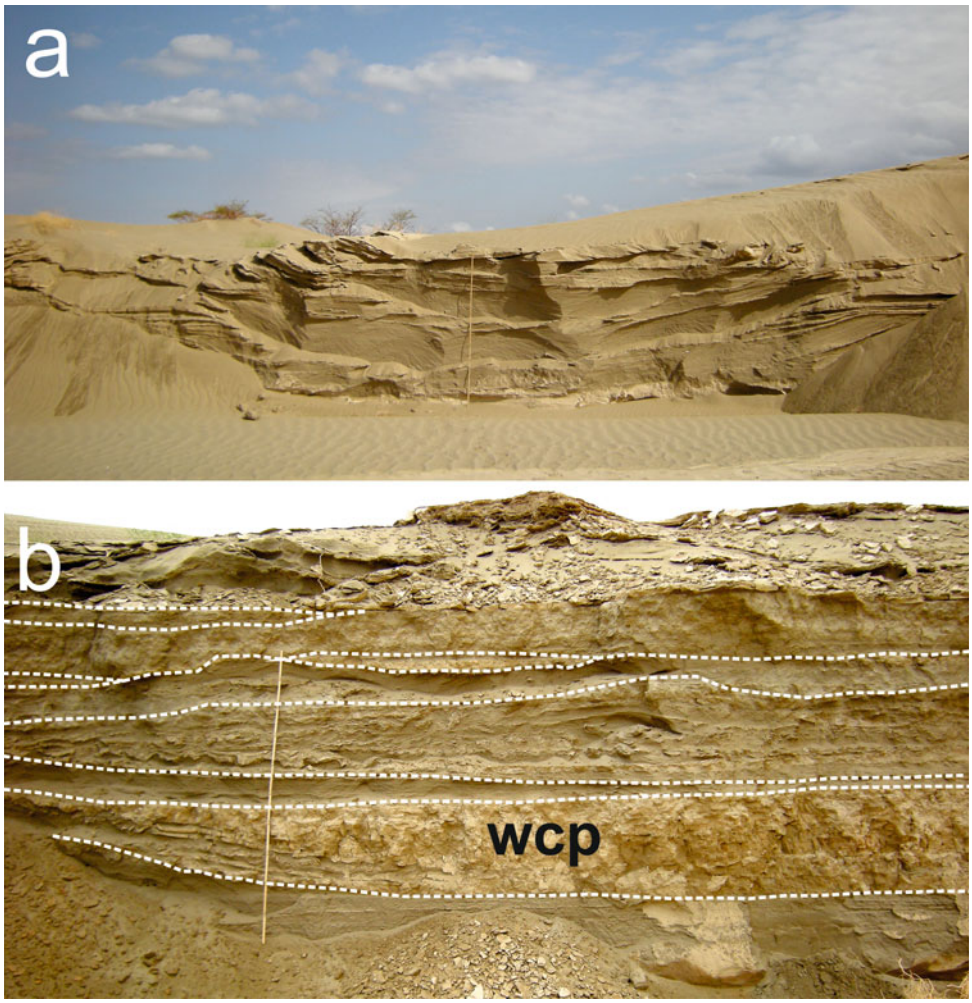

Fig. 6.27 Paleochannels in the Samoti plain filling deposit: **a** small channel (6–7 m) crossbedding; **b** large channel, about 30 m wide, with stacked old channels. wcp = weathered clay plug. The stick ruler is 2 m long

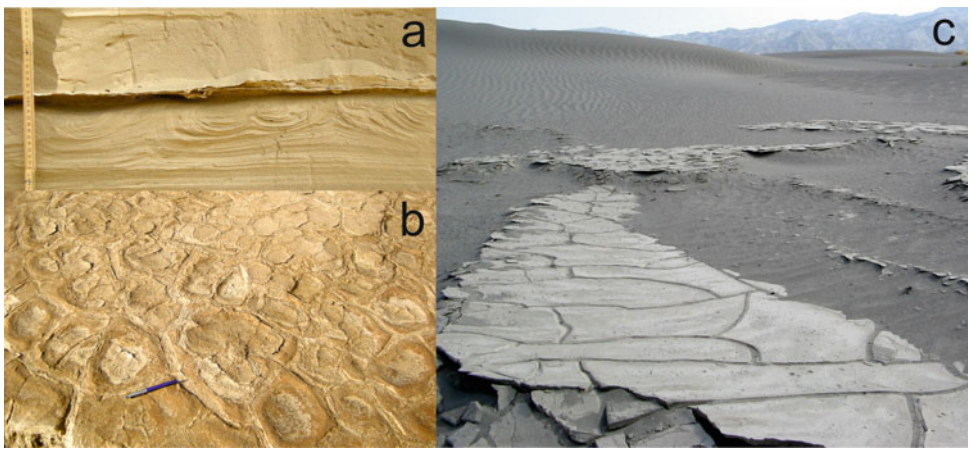

Fig. 6.28 Example of: **a** overload deformation in the infilling sedimentary sequence; **b** saturated sediment deformation of unknown origin (probably caused by overburden and/or earthquake) in the thick clay layer on top of the infilling sedimentary sequence; c) mud cracks in the thick clay layer on top of the infilling sedimentary sequence

Fig. 6.29 Foot print of a large antelope, probably a greater kudu, in the thick clay layer on top of the infilling sedimentary sequence. This animal is no longer living in the study area.

deposition of the coarser particle, whereas the sand is selectively transported farther downstream.

In the Samoti plain, wind processes are very active and a large proportion of the plain is covered with sand blown dunes. Transverse dunes, formed by the coalescing of barchan dunes, are the most common type. They are shaped by the Khamsin wind blowing from southeast. These dunes are much smaller than those of larger deserts but have a larger dune wavelength/height ratio. This may be the result of the scarce availability of sediment in the southern quadrant of the basin, which is a closed one, since the larger rivers with the higher sediment contributions enter the plain from the northeastern quadrant, whereas only very small rivers enter the plain from the southern quadrant, thus providing the Khamsin wind with supply limited conditions.

A few facts indicate that in the recent past (7–5000 years BP), the Samoti plain was subject to a wetter climate. They include:

(a) The lack of any evidence of old aeolian deposits in the exposed filling sequence
(b) The occurrence in the plain filling deposits of paleochannels as wide as the modern ones, but topped by a thick clay plug with evidence of persistent water submergence and indicating a flow depth of about 1 m. In modern rivers, instead, only a very thin (1–3 mm thick) drape may cover small parts of the streambed.
(c) Examples of saturated sediment deformations due to overload and, probably, to seismic activity are rather common in the river banks cut into the plain infilling deposits.
(d) Foot prints of a big bovidae, probably a greater kudu, were found on the thick mud layer at the top of the basin infilling sequence. This top layer is also characterized by liquefactions features and dissection cracks. Nowadays, the greater kudo lives in scrub and bush woodlands of East Africa, but it seems it is no longer present in the study area.

All these facts suggest that 7–5000 years ago, more humid conditions (African Humid Period) prevailed in the Samoti plain. The transition to a drier climate seems to have been very fast and synchronous with the structural lowering of the basin floor which caused the basin infilling incision by the northwestern rivers, while sand dunes started to form on the thick mud layer on the top of the basin infilling sequence as the climate became drier.

References

Abbate E, Albianelli A, Azzaroli A, Benvenuti M, Tesfamariam B, Bruni P, Cipriani N, Clarke RJ, Ficcarelli G, Macchiarelli R, Napoleone G, Papini M, Rook L, Sagri M, Tecle TM, Torre D, Villa I (1998) A one-million-year-old Homo cranium from the Danakil (Afar) Depression of Eritrea. Nature 393:458–460

Abbate E, Woldehaimanot B, Bruni P, Falorni P, Papini M, Sagri M, Girmay S, Tecle TM (2004) Geology of the homo-bearing Pleistocene Dandiero basin (Buia region, Eritrean Danakil depression). Riv It Paleont Strat 110(supplement):5–34

Ahlbrandt TS, Fryberger SG (1980) Sedimentary features and significance of interdune deposits. In: Ethridge FG, Flores RM (eds) Recent and ancient nonmarine depositional environments: models for exploration. Society of economic palaeontologists and mineralogists. Tulsa, Oklahoma, pp 293–314

Allen JRL (1986) Earthquake magnitude-frequency, epicentral distance, and soft-sediment deformation in sedimentary basins. Sed Geol 46:67–75

Alsop GI, Weinberger R, Levi MT (2017) Identifying soft-sediment deformation in rocks. J Struct Geol 125:248–255. https://doi.org/10.1016/j.jsg.2017.09.001

Benvenuti M, Carnicelli S, Belluomini G, Dainelli N, Di Grazia S, Ferrari GA, Iasio C, Sagri M, Ventra D, Atnafu B, Kebede S (2002) The Ziway-Shala lake basin (Main Ethiopian Rift, Ethiopia): a revision of basin evolution with special reference to the Late Quaternary. J Afr Earth Sc 35:247–269

Billi P (2007) Morphology and sediment dynamics of ephemeral streams terminal reaches in the Kobo basin (northern Welo, Ethiopia). Geomorphology 85:98–113

Costa AC, Bronstert A, de Araujo JC (2012) A channel transmission losses model for different dryland rivers. Hydrol Earth Syst Sci 16:1111–1135

de Menocal P, Ortiz J, Guilderson T, Adkins J, Sarnthein M, Baker L, Yarusinsky M (2000) Abrupt onset and termination of the African Humid Period: rapid climate responses to gradual insolation forcing. Quatern Sci Rev 19:347–361

de Menocal PB, Tierney JE (2012) Green Sahara: African humid periods paced by Earth's orbital changes. Nat Educ Knowl 3(10):12

Duffield WA, Bullen TD, Clynne MA, Fournier RO, Janik, CJ, Lanphere MA, Lowenstern J, Smith JG, Wolde Giorgis L, Kahsai G, Wolde Mariam K, Tesfai T (1997). Geothermal potential of the Alid Volcanic Center, Danakil Depression, Eritrea. US Geological Survey Open File Report 97–291, Reston

Ghinassi M, Libsekal Y, Papini M, Rook L (2009) Palaeoenvironments of the Buia Homo site: high-resolution facies analysis and

non-marine sequence stratigraphy in the Alat formation (Pleistocene Dandiero Basin, Danakil depression, Eritrea). Palaeogeogr Palaeoclimatol Palaeoecol 280:415–431
Hallet B (1990) Spatial self-organization in geomorphology: from periodic bedforms and patterned ground to scale-invariant topography. Earth-Sci Rev 29:57–76
Harvey A (2011) Daryland alluvial fans. In: Thomas DSG (ed) Arid zone geomorphology: process, form and change in drylands. Wiley, New York, pp 333–370
Holmes J, Hoelzmann P (2017)The Late Pleistocene-Holocene African Humid Period as Evident in lakes. Oxford Res Encyclop Clim Sci 1. https://doi.org/10.1093/acrefore/9780190228620.013.531
Kampf SK, Faulconer J, Shaw JR, Lefsky M, Wagenbrenner JW, Cooper DJ (2018) Rainfall thresholds for flow generation in desert ephemeral streams. Water Resour Res. https://doi.org/10.1029/2018WR023714
Lancaster N (1995) Geomorphology of desert dunes. Routledge, New York
Lancaster N (2009) Dune morphology and dynamics. In: Parsons AJ, Abrahams AD (eds) Geomorphology of desert environments, 2nd edn. Springer, Heidelberg, pp 557–596
Lancaster N (2011) Desert dune processes and dynamics. In: Thomas DSG (ed) Arid zone geomorphology: process, form and change in drylands, 3rd edn. Wiley, New York, pp 487–515
Paola C, Parker G, Seal R, Sinha SK, Southard JB, Wilcock PR (1992) Downstream fining by selective deposition in a laboratory flume. Science 258:1757–1760
Pedgley DE (1967) Air Temperature at Dallol, Ethiopia. Meteorol Mag 96:265–271
Robert A (2003) River processes. An introduction to fluvial dynamics. Arnold, London
Rosen K, Van Buskirk R, Gabresi K (1999) Wind energy potential of coastal Eritrea: an analysis of sparse wind data. Sol Energy 66 (3):201–213
Sambrook Smith GH, Ferguson RI (1995) The gravel-sand transition along river channels. J Sediment Res 65(2a):423–430
Sambrook Smith GH, Ferguson RI (1996) The gravel-sand transition: flume study of channel response to reduced slope. Geomorphology 16:147–159
Sani F, Ghinassi M, Papini M, Oms O, Finotello A (2017) Evolution of the northern tip of Afar triangle: inferences from the Quaternary succession of the Dandiero—Massawa area (Eritrea). Tectonophysics 717:339–357
Sun Q, Liu Y, Salem A, Marks L, Welc F, Ma F, Zhang W, Chen J, Jiang J, Chen Z (2019) Climate-induced discharge variations of the Nile during the Holocene: Evidence from the sediment provenance of Faiyum Basin, north Egypt. Global Planet Change 172:200–210
Tjallingii R, Claussen M, Stuut J-BW, Fohlmeister J, Jahn A, Bickert T, Lamy F, Rohl U (2008) Coherent high-and low-latitude control of the northwest African hydrological balance. Nat Geosci 1:670–675
Tooth S (2000) Process, form and change in dryland rivers: a review of recent research. Earth-Sci Rev 51:67–107
Terwilliger VJ, Eshetu Z, Huang Y, Alexandre M, Umer M, Gebru T (2011) Local variation in climate and land use during the time of the major kingdoms of the Tigray Plateau in Ethiopia and Eritrea. CATENA 85:130–143
Venditti JG, Domarad N, Church M, Rennie CD (2015) The gravel-sand transition: sediment dynamics in a diffuse extension. J Geophys Res Earth Surf 120:943–963